# ChemComm

Check for updates

# Q-Graphene-loaded metal organic framework nanocomposites with water-triggered fluorescence turn-on: fluorimetric test strips for directly sensing trace water in organic solvents†

Yuanyuan Cai, Luping Feng, Yue Hua, Huan Liu, Mengyuan Yin, Xiaoxia Lv, Shuai Li and Hua Wang [ID] *

A solid-state fluorimetric strategy has been developed using test strips coated with Q-graphene-loaded metal–organic framework nanocomposites featuring water-triggered fluorescence turn-on. It can facilitate the real-time evaluation of trace water in organic solvents, with the level down to about 0.015% in alcohol.

Water is a very important resource in nature; however, it may act as a contaminant and harmful impurity in many solvents or products in pharmaceutical, food, and chemical industries of great importance.[1,2] For example, trace water in organic chemical reactions may exert a great influence on the process of reactions, and sometimes even determine the reaction product, yield, and selectivity.[3] As a result, it is of great importance to quantify the water content in organic solvents. As another example, aviation gasoline (avgas) should be free of water for the safe operation of aircrafts.[4] In addition to the decreasing utilization efficiency of fuel, trace water in avgas may bring about horrible hazards due to the fact that it may form ice to block fuel lines, screens, or orifices in the fuel system under the harsh flying conditions.[4] Up to date, many analysis methods have been proposed mostly known as the Karl Fischer (K-F) titration methods, which perform the assays of water contents through coulometric and volumetric analyses.[5–7] This classic approach may involve skilled personnel, specialized equipment, time-consuming procedures, and incapability of continuous monitoring.[8] In particular, it is unsuitable for rapid and direct evaluation of water contents.[9–12] Therefore, exploring simple and sensitive methods for rapid and field-employable monitoring of trace water is a hot goal to pursue in the fields of pharmaceutical,[13] chemical,[2] and aircraft industries.[4]

Fluorimetric detection methods with some outstanding advantages like rapid analysis and high sensitivity have been applied as very popular analysis tools for various analyzers,[14–22] including water in organic solvents.[19–22] Nevertheless, the majority of current fluorimetric assays are performed in solutions,[19–22] which may encounter the interference of co-existing substances in the solution backgrounds especially for those using fluorescence (FL) quenching,[21,22] resulting in low detection sensitivity and selectivity. What is more, they may not be suitable for the direct and real-time evaluation of water contents in practical samples. Alternatively, some efforts have been devoted to the fabrication of solid phase-based fluorimetric analysis technologies like the ones that use test strips.[23,24] Yet, the test strip-based fluorimetric methods have hardly been reported for sensing trace water in organic solvents.

It is established that fluorimetric strategies can largely depend on the optical properties and sensing performances of fluorescent probes such as FL intensity and environmental stability. Moreover, recent years have witnessed the rapid development of metal–organic frameworks (MOFs) with high porosity, adjustable size, and controllable structure for wide applications in separation, catalysis, energy, and as luminescent sensors.[25–30] In particular, some MOFs themselves with π-conjugated structures can display favorable FL properties to act as fluorescent probes for the design of fluorimetric platforms.[16,18,22,31] For example, Yin's group reported a ratiometric FL sensor using the Ru@MIL MOF for the sensitive detection of water in organic solvents.[31] Müller-Buschbaum *et al.* developed a humidity sensor using MOFs with FL turn-off caused by water.[22] Besides, MOFs with inherent porosity and guest-binding ability can be tailored for solid-state fluorimetric strategies like test strips.

In the present work, we have developed fluorimetric test strips using Q-graphene (QG)-loaded MOF nanocomposites for the turn-on detection of trace water in organic solvents. Scheme 1 schematically illustrates the synthesis procedure of the nanocomposite probes for the test strip-based fluorimetric analysis of water. The MOF precursors Zn(NO₃)₂ and 2-aminoterephthalic acid (BDC-NH₂) were combined with amine-derivatized melamine (MA) and hollow QG scaffolds to produce the QG-loaded MOF nanocomposites through the cross-linking chemistry of glutaraldehyde (GA).

*Institute of Medicine and Materials Applied Technologies, College of Chemistry and Chemical Engineering, Qufu Normal University, Qufu City, Shandong Province 273165, P. R. China. E-mail: huawang@qfnu.edu.cn*
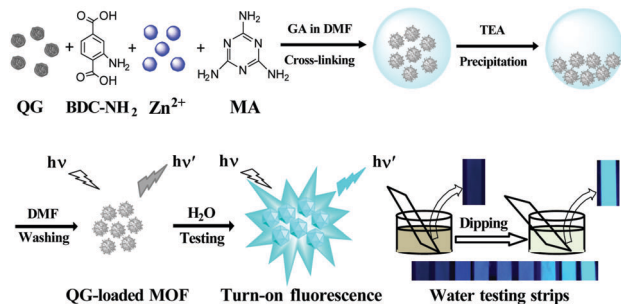
Scheme 1 Schematic illustration of the synthesis process of QG-loaded MOF nanocomposites, including GA crosslinking, TEA precipitation, and DMF washing, showing the $H_2O$-triggered fluorescence turn-on, and the fabrication procedure of water test strips for the fluorimetric detection of $H_2O$ in organic solvents.



Fig. 1 (A) FL spectra and (B) UV-vis spectra of (a) BDC-NH$_2$, and QG-loaded MOF nanocomposites (b) before and (c) after the addition of $H_2O$ in alcohol (5.0%) (inset: the photographs of the corresponding product solutions under UV or white light).

Herein, MA with three amines, whose photonic nitrogen atoms might serve as the electron donors as confirmed previously,[23,32] were employed initially aiming to increase the FL of the resulting MOFs, of which BDC-NH$_2$ itself can present blue FL because of the existence of the amine group. Meantime, QG, a special graphene material consisting of multi-layer graphene and many folded edges and surface defects,[33,34] was introduced as the scaffold to improve the environmental stability of MOFs. To our surprise, the resultant MOF nanocomposites displayed no significant FL in the organic reaction system. However, they could exhibit extremely strong blue FL once in the presence of water, which is defined as water-triggered FL turn-on. The possible mechanism was speculated to be that water might destroy the MOF nanocomposites to release fluorescent BDC-NH$_2$ and $Zn^{2+}$ ions generating ZnO in water. As a result, the BDC-NH$_2$ FL would be enhanced by the resulting ZnO as evidenced for fluorophores elsewhere,[32,35,36] which should be responsible for the FL turn-on of the system. In addition, the amine-derivative MA might further increase the FL intensity of BDC-NH$_2$ through its amines conducting the "electronic donor" effects aforementioned. The amounts of the main components of QG-loaded MOF nanocomposites were optimized to be 2.5% MA, $Zn^{2+}$-to-BDC-NH$_2$ ratio of 3.28/1, and 1.0% QG (Fig. S1, ESI†). Furthermore, the prepared QG-loaded MOF nanocomposites were coated onto filter papers to produce water test strips, which were fabricated by taking advantage of the high viscosity of MA-GA resin involved in the nanocomposites as reported previously.[37,38] A solid-state fluorimetric strategy was thus developed practically for the real-time evaluation of trace water in organic solvents (i.e., ethanol, DMF, and avgas).

The fluorimetric water responses of QG-loaded MOF nanocomposites were comparably investigated by taking the MOF precursor of BDC-NH$_2$ as the control (Fig. 1A). One can note that the QG-loaded MOF nanocomposites could present no FL spectrum (curve b), whereas BDC-NH$_2$ itself displayed blue FL (curve a). Importantly, the developed nanocomposites could light up with a FL emission at 424 nm once water is added, showing water-triggered FL turn-on (curve c), which can be visually observed from the corresponding photographs (Fig. 1A, inset). Furthermore, Fig. 1B shows the UV-vis spectra of QG-loaded MOF
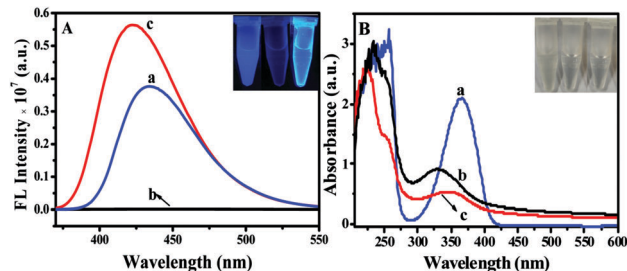
nanocomposites before and after adding water, in comparison with BDC-NH$_2$. It was found that the QG-loaded MOF nanocomposites had a UV absorption peak at 350 nm (curve b), which could display a little of absorption shift after the addition of water (curve c). Notably, the BDC-NH$_2$ precursor can itself exhibit a UV absorption peak at 370 nm (curve a), which might act as the UV-vis absorption source of the developed nanocomposites. Besides, it was observed that the MOFs prepared with BDC-NH$_2$ and $Zn^{2+}$ precursors only could also display a fluorescent emission, but showing poor aqueous stability and low FL turn-on efficiencies in sensing water.

The morphological structures of QG-loaded MOF nanocomposites were characterized before and after adding water by SEM imaging (Fig. 2). One can see from Fig. 2A that the MOF nanocomposites were well dispersed showing the spherical structure with an average size of about 100 nm in diameter. After the introduction of water, to our surprise, the spherical QG-loaded MOF nanocomposites could be transformed to flower-like particles with the uniform size of about 1.5 μm in diameter, showing a dramatic change in the structure and size (Fig. 2B). Moreover, the elemental compositions of the QG-loaded MOF nanocomposites with and without water were explored separately by energy dispersive spectroscopy (EDS) and elemental mapping analysis, with the data shown in Fig. S2, ESI.† It is noteworthy that the spherical nanocomposites can possess the elements C, N, O, and Zn with uniform distribution, indicating the successful formation of the nanocomposites (Fig. S2A, ESI†). Also, after the addition of water, the formed flower-like products can include these elements distributed in a discretely mixed way
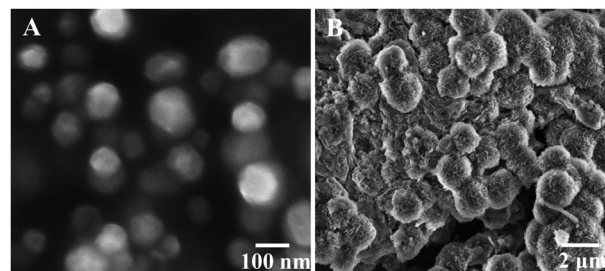


Fig. 2 SEM images of QG-loaded MOF nanocomposites in the (A) absence and (B) presence of water.

(Fig. S2B, ESI†). Accordingly, the MOF nanocomposites might retain the elemental composition in the presence of water, although their topological structures could be largely changed.

Moreover, the QG-loaded MOF nanocomposites were coated onto filter papers to fabricate the test strips for the solid-state fluorimetric sensing of water. Herein, the FL turn-on efficiencies were calculated according to the equation: FL turn-on efficiency = $(I - I_0)/I_0$, where $I_0$ and $I$ refer to the FL intensities of the QG-loaded MOF nanocomposites in the absence and presence of water, respectively. The main detection conditions of the fluorimetric test strips were optimized for sensing water in alcohol (Fig. S3, ESI†). One can see that the water-induced FL turn-on efficiencies can depend on the amounts of the QG-loaded MOF, showing that the most suitable one was obtained at the nanocomposite amount of 0.20 mg mL$^{-1}$ (Fig. S3A, ESI†). Also, the FL turn-on responses of the test strips to water were studied under different pH conditions, and the optimal pH value was obtained at pH 5.0 (Fig. S3B, ESI†). Furthermore, the maximal temperature for sensing water was determined to be at 37 °C, as revealed in Fig. S3C, ESI.† In addition, it was observed that the ionic strengths may have no significant effect on the water responses of the test strips, even the media might contain NaCl concentrations up to 300 mM (Fig. S3D, ESI†). That is, the electrostatic interaction might hardly influence the interaction between water and MOF nanocomposites coated on the test strips.

The fluorimetric sensing selectivity of the QG-loaded MOF-coated test strips was systematically explored for probing water in comparison with some common organic solvents (Fig. 3). It was found that only water could trigger the FL turn-on of the test strips, whereas the other organic solvents exhibited no FL change, as apparently shown in the corresponding photographs (Fig. 3A, inset). More importantly, the test strips could sensitively probe water co-existing separately in other organic solvents (Fig. 3B), as evidenced in the photographs of the resultant products (Fig. 3B, inset). Accordingly, the so developed water test strips could allow for the selective detection of water in various organic solvents. As aforementioned, when the test strips were dipped into water, the coated QG-loaded MOF nanocomposites would collapsed to release fluorescent BDC-NH$_2$ and produce ZnO towards the strong blue FL, in which ZnO should serve as the FL enhancer. In the meantime, the amine-containing MA present

would also contribute to the further increase in FL of BDC-NH$_2$ by the "electronic donor" effects, as previously confirmed for amine derivatives.[23,32]

The environmental robustness and storage stability of the developed water test strips were investigated by taking the MOF-coated ones without QG for comparison under harsh testing conditions (Fig. S4, ESI†). One can note that when exposed to a xenon lamp over different time intervals, the QG-loaded MOF-coated test strips could display no significant change of FL turn-on efficiencies in sensing water, whereas the MOF-coated ones could encounter with greatly decayed FL turn-on efficiencies (Fig. S4A, ESI†). Also, the storage stability of the test strips was studied (Fig. S4B, ESI†). Apparently, the QG-loaded MOF-coated test strips could basically maintain the water-response performances even stored for five months, in contrast to the MOF-coated ones showing a significant change of water sensing ability. Therefore, the QG-loaded MOF-coated test strips can possess higher environmental and storage stabilities. Herein, the use of QG scaffolds for loading MOFs would endow the nanocomposites with high environmental stability, because the hexatomic ring-containing QG should perform strong π–π stacking interaction with the benzene ring-containing BDC-NH$_2$ and MA of the nanocomposites. Besides, the nanocomposites were coated onto the test strips by the use of highly viscous MA-aldehyde resin, which could additionally ensure high environmental robustness of the test strips.

The application feasibility of the developed water test strips with QG-loaded MOF nanocomposites was investigated by separately probing water in organic solvents e.g. ethanol, DMF, and avgas (Fig. 4). Fig. 4A describes the solid-state fluorimetric results for different levels of water in ethanol, showing that the FL turn-on intensities of the test strips could rationally increase with the increase in water levels in the tested media. A calibration curve of FL turn-on efficiencies versus the percentages in volume of water in alcohol was obtained linearly ranging from 0.05% to 6.0% ($R^2$ = 0.9901), with the limit of detection (LOD) of about 0.015% estimated by the 3σ rule (Fig. 4B). Moreover, Fig. 4C illustrates a relationship between the FL turn-on efficiencies and the percentages in volume of water in DMF. Accordingly, water could be detected over a linear concentration range of 0.10–9.5% ($R^2$ = 0.9836), with the LOD of 0.030%. By comparison, the water-sensing performances of the developed test strips are much better than those of the classic Karl Fischer titration methods via coulometric and volumetric analyses[6] or most current detection methods for fluorimetric detection of water in organic solvents.[25,31] Besides, the developed water test strips were employed to evaluate water in avgas, showing that water could be quantified with the linear concentrations ranging from 0.10% to 12.0% ($R^2$ = 0.9856), with the LOD of 0.050% (Fig. 4D). These data indicate that the developed solid-state sensing strategies with fluorimetric test strips can hold great potential for practical applications for the evaluation of trace water in different organic solvents.

In summary, a solid-state fluorimetric strategy with test strips has been for the first time developed using QG-loaded
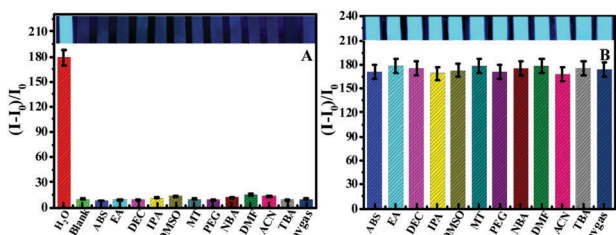


Fig. 3 The FL turn-on efficiencies of water test strips with QG-loaded MOF nanocomposites to (A) different organic solvents including blank (alcohol), ABS, EA, DEC, IPA, DMSO, MT, PEG, NBA, DMF, CAN, TBA, and avgas (5.0%), with the corresponding photographs of test strips under UV light (top), and (B) different organic solvents separately co-existing with H$_2$O (5.0%).
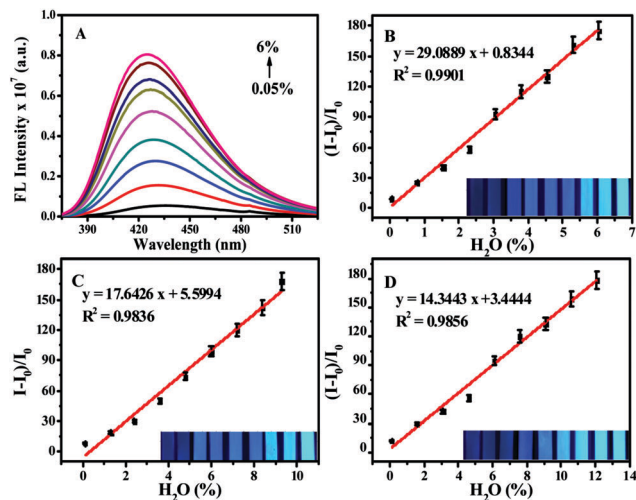
Fig. 4 (A) FL spectra of water test strips for sensing water of different percentages in alcohol, and the calibration curves of the FL turn-on efficiencies *versus* water percentages in (B) alcohol (0.050–6.0%), (C) DMF (0.10–9.3%), and (D) avgas (0.10–12.1%) (inset: the resultant photographs of water test strips under UV light).

MOF nanocomposites for the turn-on detection of trace water in organic solvents (*i.e.*, ethanol, DMF, and avgas). It was discovered that the use of QG scaffolds for loading MOF nanocomposites could enhance the environmental stability of MOF probes against any light bleaching and self-quenching in aqueous storage due to the strong π–π stacking interactions. Moreover, the amine-derivatized MA could further increase the FL intensity of BDC-NH$_2$ fluorophores through the "electronic donor" effects of amines. Furthermore, the high viscosity of MA–GA resin involved in the nanocomposites can ensure the firm coatings of porous MOF probes on the water test strips. The so developed fluorimetric turn-on test strips can allow for the rapid and field-employable monitoring of trace water in organic solvents with the level down to about 0.015% in alcohol, and the sensing performances of which are comparable or better than those of the classic Karl Fischer titration methods or most current fluorimetric detection methods. Importantly, such a novel design route of fluorimetric test strips with MOF nanocomposites showing water-triggered FL turn-on should offer the guidance for the development of various solid-state fluorimetric detectors for the evaluation of trace water, thus promising the wide practical applications in the fields of pharmaceutical, food, chemical, and aircraft industries, which should be investigated in future work. To the best of our knowledge, this is the first report on a solid-state fluorimetric method with MOF nanocomposite-coated test strips for turn-on monitoring of trace water in organic solvents.

## Conflicts of interest

There are no conflicts to declare.

## Notes and references

1  D. S. Ballantine and H. Wohltjen, *Anal. Chem.*, 1985, **58**, 2883–2885.
2  T. I. Kim and Y. Kim, *Anal. Chem.*, 2017, **89**, 3768–3772.
3  H. S. Jung, P. Verwilst, W. Y. Kim and J. S. Kim, *Chem. Soc. Rev.*, 2016, **45**, 1242–1256.
4  J. Bitten, *Anal. Chem.*, 1968, **40**, 960–962.
5  D. Richter, *Angew. Chem.*, 1935, **48**, 776.
6  Y. Y. Liang, *Anal. Chem.*, 2002, **62**, 2021–2025.
7  L. A. Frink and D. W. Armstrong, *J. Pharm. Sci.*, 2016, **105**, 2288–2292.
8  S. Grünke, *Food Control*, 2001, **12**, 419–426.
9  H. Huang and P. K. Dasgupta, *Anal. Chem.*, 1990, **62**, 1935–1942.
10  V. K. Leley, N. J. Sawarkar and L. K. Badwal, *Analyst*, 1971, **96**, 460–462.
11  A. Saraullo, P. A. Martos, J. Pawliszyn and A. Chem, *Anal. Chem.*, 1997, **69**, 1992–1998.
12  J. Rudin and D. T. Wasan, *J. Colloid Interface Sci.*, 1994, **162**, 252–253.
13  D. B. Williams and M. Lawton, *J. Org. Chem.*, 2010, **75**, 8351–8354.
14  F. Gao, F. Luo, L. Tang, L. Dai and L. Wang, *J. Lumin.*, 2008, **128**, 462–468.
15  Y. Jiang, J. Zheng, Q. Duan, L. Yang, J. Zhang, H. Zhang, J. He, H. Sun and D. Ho, *Chem. Commun.*, 2018, **54**, 7967–7970.
16  H. Zhang, J. Zhang, G. Huang, Z. Dub and H. Jiang, *Chem. Commun.*, 2014, **50**, 12069–12072.
17  N. Zhang, Y. Si, Z. Sun, L. Chen, R. Li, Y. Qiao and H. Wang, *Anal. Chem.*, 2014, **86**, 11714–11721.
18  L. Feng, Z. Sun, H. Liu, M. Liu, Y. Jiang, C. Fan, Y. Cai, S. Zhang, J. Xu and H. Wang, *Chem. Commun.*, 2017, **53**, 9466–9469.
19  H. Niu, D. Huang and C. Niu, *Sens. Actuators, B*, 2014, **192**, 812–817.
20  P. Shen, M. Li, C. Liu, W. Yang, S. Liu and C. Yang, *J. Fluoresc.*, 2016, **26**, 363–369.
21  Y. Zhang, C. Liang and S. Jiang, *New J. Chem.*, 2017, **41**, 8644–8649.
22  L. V. Meyer, F. Schonfeld, A. Zurawski, M. Mai, C. Feldmann and K. Muller-Buschbaum, *Dalton Trans.*, 2015, **44**, 4070–4079.
23  Y. Qiao, J. Shang, S. Li, L. Feng, Y. Jiang, Z. Duan, X. Lv, C. Zhang, T. Yao, Z. Dong, Y. Zhang and H. Wang, *Sci. Rep.*, 2016, **6**, 36494.
24  Z. Duan, Y. Yin, C. Zhang, G. Song, S. Zhao, F. Yang, L. Feng, C. Fan, S. Zhu and H. Wang, *Analyst*, 2018, **143**, 392–395.
25  A. Douvali, A. C. Tsipis, S. V. Eliseeva, S. Petoud, G. S. Papaefstathiou, C. D. Malliakas, I. Papadas, G. S. Armatas, I. Margiolaki, M. G. Kanatzidis, T. Lazarides and M. J. Manos, *Angew. Chem.*, 2015, **54**, 1651–1656.
26  L. Chen, J. Ye, H. Wang, M. Pan, S. Yin, Z. Wei, L. Zhang, K. Wu, Y. Fan1 and C. Su, *Nat. Commun.*, 2017, **8**, 1–10.
27  D. Y. Ahn, D. Y. Lee, C. Y. Shin, H. T. Bui, N. K. Shrestha, L. Giebeler, Y. Y. Noh and S. H. Han, *ACS Appl. Mater. Interfaces*, 2017, **9**, 12930–12935.
28  M. Wang, L. Guo and D. Cao, *Sens. Actuators, B*, 2018, **256**, 839–845.
29  J. Xiao, Y. Wu, M. Li, B. Y. Liu, X. C. Huang and D. Li, *Chemistry*, 2013, **19**, 1891–1895.
30  Y. Ooyama, T. Sumomogi, T. Nagano, K. Kushimoto, K. Komaguchi, I. Imae and Y. Harima, *Org. Biomol. Chem.*, 2011, **9**, 1314–1316.
31  H. Q. Yin, J. C. Yang and X. B. Yin, *Anal. Chem.*, 2017, **89**, 13434–13440.
32  S. Li, Z. Sun, R. Li, M. Dong, L. Zhang, W. Qi, X. Zhang and H. Wang, *Sci. Rep.*, 2015, **5**, 8475.
33  E. P. Randviir, D. A. Brownson, M. Gomez-Mingot, D. K. Kampouris, J. Iniesta and C. E. Banks, *Nanoscale*, 2012, **4**, 6470–6480.
34  M. Dong, C. Liu, S. Li, R. Li, Y. Qiao, L. Zhang, W. Wei, W. Qi and H. Wang, *Sens. Actuators, B*, 2016, **232**, 234–242.
35  A. Dorfman, N. Kumar and J. Hahm, *Adv. Mater.*, 2006, **18**, 2685–2690.
36  W. Hu, Y. Liu, H. Yang, X. Zhou and C. M. Li, *Biosens. Bioelectron.*, 2011, **26**, 3683–3687.
37  A. Sowmya and S. Meenakshi, *Int. J. Biol. Macromol.*, 2014, **64**, 224–232.
38  R. Saleem, A. Adnan and F. A. Qureshi, *Indian J. Chem. Technol.*, 2015, **22**, 48–55.